

**Universality of multiparticle production in QCD at high energies**

Fabio Dominguez

*Institut de Physique Théorique, CEA-Saclay, F-91191 Gif-sur-Yvette, France*

Cyrille Marquet

*Physics department, Theory Unit, CERN, CH-1211 Geneva, Switzerland and Departamento de Física de Partículas and IGFAE, Universidade de Santiago de Compostela, 15782 Santiago de Compostela, Spain*

Anna M. Stasto

*Department of Physics, Pennsylvania State University, University Park, Pennsylvania 16802, USA; Brookhaven National Laboratory, RIKEN BNL Research Center, Building 510A, Upton, New York 11973, USA, and H. Niewodniczański Institute of Nuclear Physics, Polish Academy of Sciences, Kraków 31-342, Poland*

Bo-Wen Xiao

*Institute of Particle Physics, Central China Normal University, Wuhan 430079, China and Department of Physics, Pennsylvania State University, University Park, Pennsylvania 16802, USA*

(Received 5 October 2012; published 4 February 2013)

By studying the color structure of multiparticle production processes in  $p + A$ -type (dilute-dense) collisions, we find that higher-point functions beyond typical dipoles and quadrupoles, e.g., sextupoles, octupoles, etc., naturally appear in the cross sections, but are explicitly suppressed in the large- $N_c$  limit. We evaluate the sextupole in the McLerran-Venugopalan model and find that, in general, its analytical form cannot be written as combination of dipoles and quadrupoles. Within the color glass condensate framework, we present a proof that in the large- $N_c$  limit, all multiparticle production processes in the collision of a dilute system off a dense system can, up to all orders in  $\alpha_s$ , be described in terms of only dipoles and quadrupoles.

DOI: [10.1103/PhysRevD.87.034007](https://doi.org/10.1103/PhysRevD.87.034007)

PACS numbers: 24.85.+p, 12.38.Cy, 13.85.Hd

**I. INTRODUCTION**

Calculating cross sections for multiparticle (multijet) production processes can be theoretically challenging when a resummation of multiple interactions is needed, as is the case in large parton density environments such as the small- $x$  regime accessible in high-energy nuclear collisions. The main complication comes from the fact that partons scatter coherently and cannot be regarded separately. In particular, it is very important to appropriately consider the color structure of the multiparticle states since color conservation plays an important role as a source of correlations.

The standard way of calculating such multiple-scattering processes is to consider the small- $x$  gluons as an external field where high-energy probes scatter in an eikonal way (see Ref. [1]). Under that framework, each parton traversing the field contributes to the scattering amplitude with a Wilson line in the appropriate representation (fundamental for quarks, adjoint for gluons) at a fixed transverse coordinate. Provided they are put together in the correct order, the Wilson lines account for the color flow of the process under consideration. After averaging (summing) over initial (final) colors at the cross-section level, one is left with a product of traces involving Wilson lines in the fundamental representation and color matrices which are contracted with adjoint Wilson lines.

These adjoint Wilson lines can be subsequently replaced by two fundamental Wilson lines by means of the identity

$$W^{ab}(x) = 2 \text{Tr}[t^a U(x) t^b U^\dagger(x)], \quad (1)$$

where  $W(x)$  stands for a Wilson line in the adjoint representation at a fixed transverse coordinate,  $U(x)$  is the corresponding Wilson line in the fundamental representation, and  $t^a$  are color matrices in the fundamental representation as well. The color matrices can be removed using the Fierz identity  $t_{ij}^a t_{kl}^a = \frac{1}{2} \delta_{il} \delta_{jk} - \frac{1}{2N_c} \delta_{ij} \delta_{kl}$ . After these manipulations one is left with a sum of products of traces of Wilson lines in the fundamental representation only.

In order to calculate measurable observables in this framework, including cross sections for multiparticle production, it is necessary to take a weighted average over the possible external field configurations. This averaging process introduces nontrivial correlations between the fields entering the different Wilson lines, therefore giving rise to the aforementioned coherent scattering involving possibly all of the partons appearing in the process. The physics encoded in this field average is inherently nonperturbative and therefore it is necessary to adopt a suitable model to be able to obtain quantitative results. Nevertheless, some features of the averaging process, such as the rapidity dependence in the low- $x$  region, can be appropriately

accounted for by perturbative considerations under the color glass condensate framework [2].

Regardless of the model under consideration, for the specific calculation of such field averages the complexity of the calculation of higher-point correlators increases accordingly with the number of Wilson lines involved. In the same way, the evolution equations derived perturbatively become very cumbersome and not well-suited for numerical evaluations. The first step in an attempt to simplify the treatment of such higher-point correlators is to consider the large- $N_c$  limit, in which the average of a product of traces of Wilson lines reduces to a product of averages involving only one trace at a time. In other words, correlations involving fields coming from Wilson lines from different traces are suppressed by factors of  $N_c$ .

Now, in this large- $N_c$  limit it becomes necessary to appropriately count the factors of  $N_c$  coming from these multiple-scattering terms and keep only the leading terms in such an expansion. Once all the color matrices (fundamental or adjoint) from vertex contributions have been removed by means of the proper color identities, the power of  $N_c$  associated to a given term is just the number of color traces involved.

In principle, all sorts of correlations involving multiple Wilson lines at various transverse coordinates can appear when considering the cross section of a multiparticle production process, but when the large- $N_c$  limit is taken only a few of those contributions are important. Taking into account the way that powers of  $N_c$  appear from the correlators, it is not difficult to realize that the terms with simpler structure are the ones that contribute the most. For a given process, the number and identity (quark or gluon) of the particles in the final state determines the maximum number of Wilson lines present in the multiple-scattering terms. The maximum power of  $N_c$  present in such terms will correspond to the configuration in which all the Wilson lines can be grouped in as many traces as possible, therefore favoring terms with traces of only a few Wilson lines.

As a first guess, one could suggest that this  $N_c$  power counting implies that the leading  $N_c$  contribution always comes from a term which only includes color dipole amplitudes (traces of two Wilson lines) and therefore has a maximal number of color traces. This guess has been proven wrong since thorough studies of two-particle production processes [3–5] have shown that some processes do not admit a description in terms of only color dipoles, but that in addition color quadrupoles (traces of four Wilson lines) are involved as well in the large- $N_c$  limit. This quadrupole amplitude cannot in general be written in terms of dipole amplitudes only and its small- $x$  evolution is determined by an independent equation as shown in Refs. [3,6,7]. It has also been shown that there is a direct relation between this quadrupole amplitude and the so-called Weiszäcker-Williams unintegrated gluon distribution function [5].

More complicated correlators naturally arise in the calculation of cross sections of processes with more particles in the final state, but they are suppressed by powers of  $N_c$  as compared with terms with only dipole and quadrupole amplitudes. They are nevertheless independent from the dipole and quadrupole amplitudes and in principle should be evaluated on their own. A procedure to evaluate higher-point correlators—in a Gaussian model in the large- $N_c$  limit—is described in the Appendix, and the explicit example of a correlator of six Wilson lines is evaluated explicitly. The small- $x$  evolution of such correlators was recently studied analytically in Ref. [8] and numerically in Ref. [9]; the evaluation shown in the Appendix provides a suitable initial condition for such equations.

The main purpose of this paper is to show that, in the large- $N_c$  limit, all multiparticle production processes considered under this framework can be described in terms of only dipoles and quadrupoles. We first work out explicitly examples with three particles in the final state before proceeding to prove the general statement by induction in the number of particles in the final state. The inductive step is greatly simplified by the observation that it is not necessary to consider all the diagrams contributing to a given process; rather, one only needs to find at least one diagram with a term given only by dipoles and quadrupoles which dominates in the large- $N_c$  limit.

## II. GENERAL CONSIDERATIONS

For definiteness' sake, let us be more specific about the scenario which we are explicitly considering. We are interested in processes where multiparticle production takes place in the presence of a (strong) background field where a highly energetic initial parton (photon, quark, or gluon) undergoes multiple scatterings. This scenario is particularly well-suited for nuclear deep inelastic scattering (DIS) experiments and forward particle production in proton-nucleus collisions (using collinear factorization for the proton) where the high-density effects of the target are encoded in the background field. For this particular case the situation simplifies even more since the coherence times of the produced particles are long compared with the length of the target nucleus and therefore the multiple interaction with the dense system can be considered as instantaneous. The process is then regarded as an incoming high-energy parton which splits several times into a given final multiparticle state, interacting at given time with the target which induces a color rotation in the whole multiparticle system [see Fig. 1(a)]. Of course, one has to consider the scattering with the target happening at all possible stages of the splitting process and sum all of these contributions, but for the counting of powers of  $N_c$ , which is of our interest, this does not make a difference.

The  $N_c$  power counting can only be done at the level of the cross section after one has already averaged (summed) over initial (final) colors. Nevertheless, one can make some

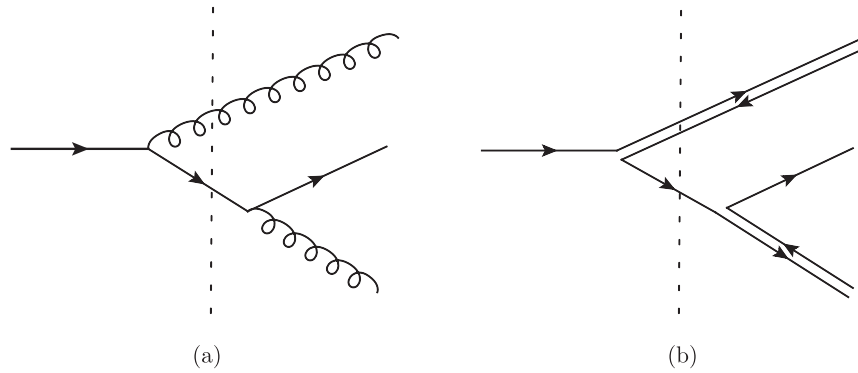


FIG. 1. Diagram contributing to the process  $q \rightarrow qgg$ . The dotted line represents the multiple scattering with the target. (a) Sample diagram. (b) Sample diagram in the large- $N_c$  limit.

general observations at the level of the amplitude based on color conservation. For a fixed process, with a specific parton in the initial state and a definite particle content in the final state, it is possible to determine the maximum number of color traces one can have in the description of the process in the leading order. Take a diagram for such a process at tree level in the large- $N_c$  limit, replacing all gluon lines with double quark-antiquark lines which make the color flow explicit, as in Fig. 1(b). As a consequence of color conservation each of the external fermion lines must be connected to another and, since we are considering only tree-level diagrams for the moment, there are no closed loops. From this observation we can see immediately that the maximal number of color traces at tree level is given by the total number of external fermion lines divided by two (with each external gluon contributing two fermion lines). Furthermore, one can see that this maximal number of traces is realized when one considers the square of a given diagram, while interference terms involving different diagrams on the amplitude and conjugate amplitude can possibly have less color traces.

Also illustrated in Fig. 1(b) is the fact that each fermion line appears at most twice at the moment of the multiple scattering, regardless of the exact position of the scattering with respect to the splittings. As a consequence, at most two fundamental Wilson lines are color connected at the amplitude level and therefore, when considering the amplitude squared, the respective color traces in the cross section would have only two Wilson lines (dipoles) or

four Wilson lines (quadrupoles). The same will be true for any term with the maximal number of traces.

Diagrams like those in Fig. 1 are useful for visualizing the branching of the initial parton into the multiparticle final state but do not contain all of the information needed to resolve the color structure of the different contributions to the cross section. For that purpose it is necessary to consider diagrams including the amplitude and the conjugate amplitude where one can perform the necessary color sums and averages. As an example, let us consider the simple process of a quark splitting into a quark and a gluon which then scatters with a background field. By putting the amplitude and the conjugate amplitude in the same diagram we obtain Fig. 2(a), where the dotted lines represent the moment of the scattering in both the amplitude and conjugate amplitude and the dashed line in the middle represents the final state at  $t = \infty$ . Since the approach employed here makes explicit use of the eikonal approximation to account for the multiple scattering with the external field, it is necessary to consider these diagrams in a coordinate representation where each particle has a definite transverse coordinate. All particles in the final state which are to be detected, and therefore would have a fixed transverse momentum, have different transverse coordinates on each side of the cut at  $t = \infty$ . When considered in the large- $N_c$  limit, one can see in Fig. 2(b) how some of the fermion lines close into loops, which will contribute one color trace to the cross section, while other lines remain open due to the fact that they contain particles in

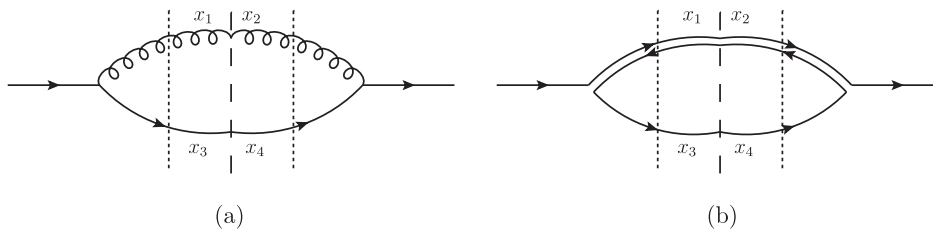


FIG. 2. Diagrams with the amplitude and conjugate amplitude for the process  $q \rightarrow qg$ . (a)  $q \rightarrow qg$ . (b)  $q \rightarrow qg$  in the large- $N_c$  limit.

the initial state. These particles in the initial state should be color connected on both sides of the diagram since one averages over initial colors at the level of the cross section, but such a connection is not explicit in this kind of diagram.

If one is interested in the color structure only, then it is more convenient to draw one fermion loop for each color trace and gluon lines for each adjoint index contraction (including adjoint Wilson lines too). This can be easily achieved by folding the corresponding diagram with the amplitude and conjugate amplitude on itself in such a way that the color connections of the initial state are made explicit. Also, in order to be able to visualize in the diagram which are the Wilson lines entering the expression of the cross section, we will stretch the lines involved in the scattering (both in the amplitude and conjugate amplitude) in the horizontal direction, and use the other lines only to illustrate the color connections. For example, the diagram corresponding to Fig. 2(a) is shown in the left-hand side of Fig. 3. One can go one step further and replace all of the gluon lines by double fermion lines using the corresponding color identity—which has the graphical representation depicted in Fig. 4—in which case the example above takes the form shown in the right-hand side of Fig. 3. Let us focus on the first term—which is the one surviving in the large- $N_c$  limit—where one can identify right away two pieces which are color disconnected, each contributing a color trace to the cross section. One involves two Wilson lines, and therefore is a dipole, while the other involves four, and therefore is a quadrupole.

The example above shows how this graphic approach allows us to easily recognize which kinds of correlators come into the expression for the cross section of a given process. One can also recognize that the combination of Wilson lines describing such a multiple scattering is given by

$$\text{Tr}[U_3 U_4^\dagger t^a t^b] W_1^{ac} W_2^{\dagger cb} = \frac{1}{2} \text{Tr}[U_1 U_2^\dagger U_3 U_4^\dagger] \text{Tr}[U_1^\dagger U_2] - \frac{1}{2N_c} \text{Tr}[U_3 U_4^\dagger], \quad (2)$$

where Fierz identities were used to reach the right-hand side. For more complicated processes the color algebra can be very cumbersome, and we will rely heavily on the graphic approach to be able to identify the leading  $N_c$  piece of the diagrams involved. In particular, it will be

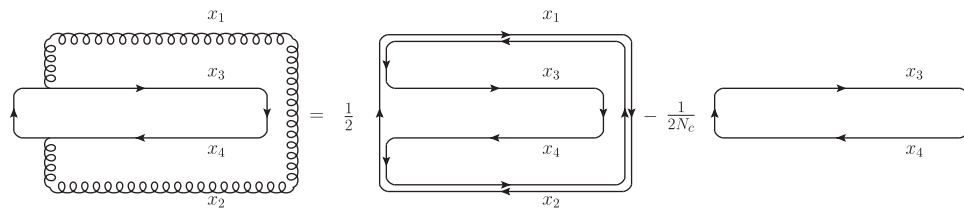


FIG. 3. Alternative representation for the process  $q \rightarrow qg$ .

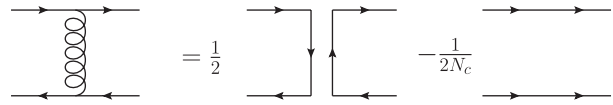


FIG. 4. Graphical representation of the Fierz identity.

crucial to identify the pieces corresponding to dipoles and quadrupoles, which we show separately in Fig. 5.

It was also mentioned earlier that one should sum over all of the possibilities for the multiple interaction to take place in the amplitude and the conjugate amplitude. Consider the process in the example above but with the multiple interaction occurring in the conjugate amplitude before the splitting. Figure 6 illustrates how the different diagrams explained above look for this variation of the same process. For this particular case it is clear that the contribution to the cross section can be written in terms of two dipoles. This example illustrates a very important fact that will allow us to concentrate on a smaller number of diagrams: changing the position of the multiple scattering might change the number of Wilson lines appearing in the corresponding term in the cross section, but it does not change the number of color traces. It might happen that for some particular cases a color trace is left with no Wilson lines inside, giving a trivial factor of  $N_c$ , but what is important is that the counting of powers of  $N_c$  is the same for a given process regardless of the position of the multiple scattering with respect to the splittings.

The last consideration to be noted before beginning a detailed explanation of particular cases is the effect of integrating out particles in the final state. In order to consider inclusive processes it is sometimes necessary to integrate over the momenta of outgoing particles that are not explicitly measured. This happens at the leading order for processes in which one produces an additional fermion in the final state without its corresponding antiparticle; for example, in single inclusive deep inelastic scattering where the incoming photon splits into a quark-antiquark pair, but only one of them is measured in the final state. For all other processes this effect comes in at next-to-leading order and will be fundamental if we want our proof to be complete to all orders.

Under the eikonal approximation at work in this formalism, the multiple-scattering terms take the form of simple Wilson lines in the appropriate representation only when considering the process in transverse coordinate space.



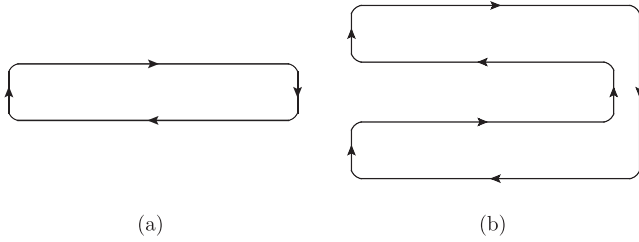


FIG. 5. Graphical representation of the two amplitudes to be used throughout the paper. (a) Dipole amplitude. (b) Quadrupole amplitude.

The momenta of the particles of the final state then enters through a Fourier transform of the respective coordinate in the amplitude and conjugate amplitude. Therefore integrating over the transverse momentum of a particle in the final state gives a delta function which identifies the transverse coordinate of the particle in the amplitude with the one in the conjugate amplitude. Given the unitarity of the Wilson lines, this sort of manipulation will likely reduce the number of Wilson lines appearing in the corresponding contribution to the cross section of any particular diagram. The sum over color indices in the final state guarantees that if a final-state particle participates in the multiple scattering both in the amplitude and the conjugate amplitude, both Wilson lines appear next to each other in the contribution to the cross section, and if they are placed at the same transverse coordinate then they exactly cancel out. This sort of cancellation between real and virtual contributions for final-state interactions has been studied before, and it is well-known to be an immediate consequence of unitarity [10]; the only place where interactions with the unmeasured particle come in is in the interference terms between initial- and final-state interactions.

From the point of view of the correlators we are interested in, it is clear that the ones entering the cross sections of these more inclusive processes are either the same or simpler than the ones involved in the expression for the full exclusive process where all particles in the final state are detected. This observation allows us to focus our attention to the fully exclusive processes only.

### III. KNOWN CASES: ONE AND TWO PARTICLES IN THE FINAL STATE

Since our goal is to prove by induction a statement that will be valid for all multiparticle production processes in

the previously described setup, it is necessary to start our analysis with the simplest cases available. All of these cases have been previously studied in the literature; here we comment on the results and emphasize the features of the derivations which will be useful for the development of the argument for general cases.

We start with processes with one particle in the final state even though their color structure is better understood in the context of processes with two particles in the final state. The reason for this is that the nontrivial contributions to these processes are obtained after integrating out one of the particles in the final state. As explained in the previous section, this procedure yields simpler expressions where the correlators appearing in the cross section have less Wilson lines than the corresponding correlators for the processes with two final-state particles. The choice to present the one-particle processes first follows the thread of the main idea, where we intend to organize the processes in terms of the number of particles in the final state; from there on the emphasis will be put on fully exclusive processes with less exclusive processes already accounted for by the observations of the previous section.

#### A. SIDIS

Semi-inclusive deep inelastic scattering (SIDIS) has been widely studied in the literature since it has been recognized as giving access to transverse momentum-dependent parton distribution functions. In the context of saturation physics, several studies have cemented the foundations of the formalism to treat deep inelastic scattering processes where the focus was mainly on the total cross section and form factors. Most of these studies are based on the dipole model approach [11], which shows directly a clear relation between the total cross section and the forward amplitude of a color dipole going through a background color field, but the same conclusions can be found from the setup explained in the previous sections after one integrates out all the particles in the final state. For the particular case of SIDIS, it was explicitly shown in Refs. [12–14] that the only correlator needed in the expression of the cross section is the dipole amplitude, and in Ref. [15] a direct connection to the transverse momentum-dependent quark distributions was made.

The lowest-order calculation of this process is very simple from the point of view of multiple scattering, which we are interested in here. It can be shown that for a DIS

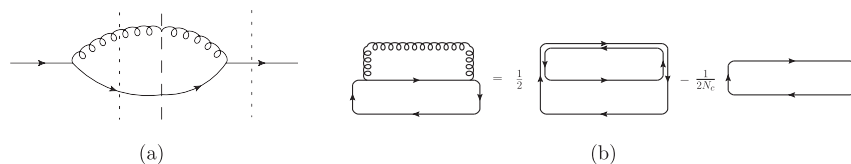


FIG. 6. Diagrams for the interference term with interaction after the splitting in the amplitude and before the splitting in the conjugate amplitude. (a) Interference term. (b) Color structure.

process—in which one considers a virtual photon splitting into a quark-antiquark pair—the multiple scattering term at the amplitude level always appears as  $1 - U(x_1)U^\dagger(x_2)$ , where  $x_1$  and  $x_2$  are the transverse positions of the quark and antiquark, respectively. Clearly, the square of this amplitude will have terms with traces of either zero, two, or four Wilson lines, but since one integrates over the momentum of one of the particles, two of the Wilson lines are at the same transverse coordinate and therefore cancel out in the term with four Wilson lines.

We note that, by swapping the initial-state photon and the quark (or antiquark) in the final state whose momentum is integrated out, the SIDIS process turns into photon + hadron production in  $p + A$  collisions (whether the photon is measured or not doesn't matter because it does not multiply scatter with the gluons of the target). Therefore the only correlator needed to express the cross section is also the dipole amplitude.

### B. Single-hadron production in $pA$

This process is of particular importance in the context of the study of cold-nuclear-matter effects. One of the first measurements to show deviations from the purely additive scheme where a nucleus is considered as an uncorrelated ensemble of nucleons was the  $p_\perp$  spectrum of produced hadrons in a proton(deuteron)-nucleus collision. Several measurements of the nuclear modification factor for inclusive hadron production were performed, showing a clear enhancement at mid-rapidities and suppression at forward rapidities [16,17], which cannot be understood without coherent scattering involving several participants in the nucleus.

In the framework described in this paper, the lowest-order contribution to this process is straightforward to calculate as the convolution of a quark distribution for the projectile with a dipole amplitude formed by the Wilson lines corresponding to the quark in the amplitude and the conjugate amplitude. At the partonic level this is simply the transverse momentum broadening of a quark going through a nucleus [18]. This level of the calculation has been proven to not be enough to describe the available data, and therefore it is necessary to consider additional contributions to the cross section coming mainly from gluon emissions, with the additional complication of having more particles in the final state. As a first attempt, it was shown in Refs. [19,20] that one can easily calculate the soft-gluon limit where the longitudinal momentum of the gluon is much smaller than that of the original quark and, therefore, the parent quark does not feel any recoil effect after the emission. This no-recoil condition is present in the transverse coordinate-space formalism in the form of the parent quark having the same transverse coordinate before and after the emission of the gluon, providing an easy way to rewrite the interference terms between scattering before and after the splitting in terms of only gluon dipoles

[1,21,22]. The details of how this manipulation works out in the Wilson-line language will be postponed to the section on dijet production.

The soft-gluon approximation implies a large rapidity gap between the measured hadron and the remnants of the proton in the forward region. In order to extend the region where the calculation is applicable, and in particular include hadrons in the forward region where the effects of saturation are expected to be stronger, it is necessary to consider the full vertex and allow the parent quark to have different transverse positions before and after the emission. This was first done in Ref. [23], where the emission vertex was treated exactly but only the divergent pieces are kept after integrating over the momentum of one of the final-state particles. These divergent pieces are shown to be absorbed by the parton distribution functions and fragmentation functions attached to the initial- and final-state partons by considering the fully Dokshitzer–Gribov–Lipatov–Altarelli–Parisi-evolved distributions. In Ref. [24], an additional contribution to the cross section—formally of next-to-leading order (NLO) but nevertheless important to restore the correct high- $p_T$  limit—was calculated. The complete NLO calculation, including the calculation of all virtual terms and also the finite terms after integration over one of the outgoing momenta, was recently done in Ref. [25]. In all cases it can be seen that, in the large- $N_c$  limit, only dipole amplitudes are needed in the full expression for the cross section. In terms of the small- $x$  evolution at NLO, the same conclusion also holds [26]. In addition, it has been demonstrated in Ref. [26] that the dipole formalism employed in this calculation holds at next-to-leading order accuracy.

As a matter of fact, one can use induction to prove that, for any single inclusive processes in terms of any order in  $\alpha_s$ , the scattering amplitudes only contain dipole amplitudes in the large- $N_c$  limit. As discussed earlier, the above conclusion holds up to leading order and NLO for  $pA$  collisions. To obtain the contribution at next-to-next-to-leading order, one just needs to add one more gluon with one single coordinate among the dipoles at the previous order (NLO). Using the Fierz identity, one can easily prove that all the relevant graphs can be reduced to products of dipole amplitudes at next-to-next-to-leading order in the large- $N_c$  limit. The proof for single inclusive DIS productions is identical. Therefore, we can conclude that all single inclusive processes can be universally described by the dipole amplitudes at the large- $N_c$  limit. From the universality point of view, the large- $N_c$  limit plays an important and indispensable role for the factorization proof. As shown in Ref. [25], higher-point functions—which are new objects—contribute to the cross sections as large- $N_c$  corrections. Without the large- $N_c$  limit, there is no universality, and hence no factorization for single inclusive processes.

### C. Dijet production in DIS

The process of dijet production in DIS is of particular interest to us since it is the simplest process where the quadrupole is needed for an accurate description of the multiple-scattering factors entering the expression for the cross section. It was carefully studied in Refs. [5,27], where its direct relation to the Weizsäcker-Williams gluon distribution function was also emphasized.

It was already mentioned in Sec. III A and previously in Refs. [5,27,28] that, to leading order at the amplitude level, the corresponding multiple-scattering factor for a process including a photon splitting into a quark-antiquark pair is given by  $1 - U(x_1)U^\dagger(x_2)$ , where  $x_1$  and  $x_2$  are the transverse positions of the quark and antiquark, respectively. Since for the dijet process one is interested in keeping the momentum variables for both particles explicit, the transverse coordinates in the amplitude and conjugate amplitude are different and therefore there is a term with four Wilson lines in the expression for the cross section. This quadrupole term takes the form  $\langle \text{Tr}[U(x_1)U^\dagger(x_2)U(x'_2)U^\dagger(x'_1)] \rangle$ , and clearly corresponds to the contribution from the diagram where the interaction with the background field occurs after the splitting in both the amplitude and conjugate amplitude. Figure 7 shows the two ways of graphically representing this process as indicated in Sec. II.

### D. Dijet production in $pA$

Processes with two particles in the final state of a proton-nucleus collision have become increasingly important in the last few years given the availability of new data and the unique character of the physics that can be probed through these particular sorts of measurements. By constraining the kinematics of the two outgoing particles, one can, at leading order, separately fix the longitudinal momentum fractions carried by the incoming partons (up to the additional fragmentation integrals involved in the case of di-hadron production), something that cannot be achieved by one-particle measurements. This advantage makes this kind of process a very attractive method to try to measure high-density effects characteristic of the small- $x$  part of the target wave function, and in fact the Relativistic

Heavy-Ion Collider measurement of di-hadron correlations in the forward region [29,30] is considered to be the strongest evidence to date of saturation.

Several studies concerning this kind of process are available in the literature, which include the role of quark distributions [31], general descriptions on how to calculate the cross sections in the presence of background fields [3,4,32,33], more phenomenological applications—including small- $x$  evolution—which make direct contact with data [34–36], and factorization studies where a direct relationship is established between these observables and unintegrated gluon distributions [5]. Here we will just present a summary of the correlators appearing in the cross section for each of these processes and the specific form they take in the large- $N_c$  limit.

The first case to be considered is the quark-initiated process, where a quark from the projectile splits into a quark and a gluon that are both detected in the final state. This is precisely the process chosen in Sec. II as an illustration of the sort of analysis to be performed throughout this paper. There it was shown how all of the terms entering the cross section for that process at leading order in the large- $N_c$  limit involve only the dipole and quadrupole correlators.

Now we turn our attention to processes with gluons in the initial state. The first one to be considered is the case where an initial gluon from the projectile splits into a quark-antiquark pair. The color algebra for this process in the large- $N_c$  limit is particularly simple since the cross section can be written in terms of only dipole correlators; nevertheless, it is important to look closely at some of the aspects of this process since it will allow us to draw general conclusions about any process with quark-antiquark pairs in the final state. The key aspect here is that the splitting does not introduce any additional color flow in the large- $N_c$  limit: in the double-line notation introduced for the large- $N_c$  limit the only effect of such a vertex is to separate the two lines and allow for different transverse coordinates for the quark and the antiquark. Such a separation has no consequences in the trace structure of the leading part of the diagram when written entirely in terms of fundamental Wilson lines.

The observation above can be easily illustrated when one compares the different contributions to the  $g \rightarrow q\bar{q}$

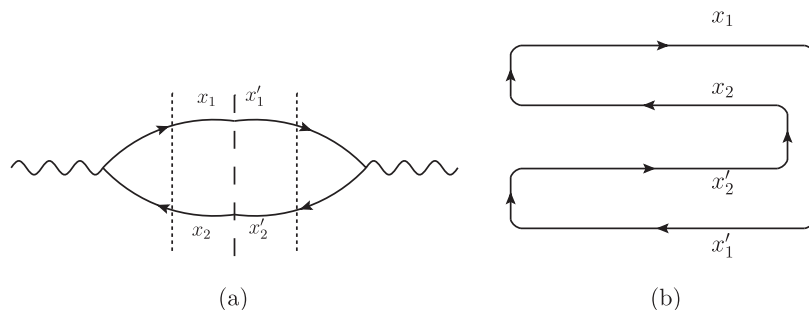
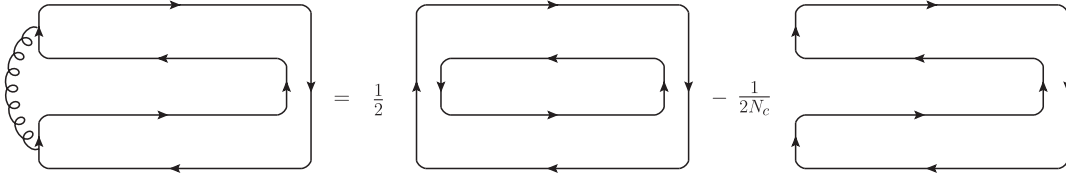


FIG. 7. Diagrams for the quadrupole term in the dijet production in DIS. The photon is omitted in (b) since we are interested only in the color structure. (a) Amplitude squared. (b) Color structure.

FIG. 8. Color structure of the  $g \rightarrow q\bar{q}$  process with interaction after the splitting.

process arising from having the multiple scattering before or after the splitting. For definiteness, consider first the case where the scattering occurs after the splitting in both the amplitude and in the conjugate amplitude. The partons involved in the scattering are therefore two quark-antiquark pairs, as indicated on the left-hand side of Fig. 8. This multiple scattering term is written in terms of Wilson lines (after averaging over the initial color of the gluon) as  $\text{Tr}[U_1 t^a U_2^\dagger U_3 t^a U_4^\dagger]$ . Using the Fierz identity to get rid of the color matrices one obtains

$$\begin{aligned} \text{Tr}[U_1 t^a U_2^\dagger U_3 t^a U_4^\dagger] &= \frac{1}{2} \text{Tr}[U_1 U_4^\dagger] \text{Tr}[U_2^\dagger U_3] \\ &\quad - \frac{1}{2N_c} \text{Tr}[U_1 U_2^\dagger U_3 U_4^\dagger]. \end{aligned} \quad (3)$$

This relation is represented graphically in Fig. 8. Now consider the case where the interaction occurs after the splitting in the amplitude and before the splitting in the conjugate amplitude. Then, the partons involved in the scattering are a quark-antiquark pair and a gluon, and the multiple-scattering factor—in terms of the corresponding Wilson lines—is

$$\begin{aligned} \text{Tr}[U_1 t^a U_2^\dagger t^b] W_3^{ba} &= \frac{1}{2} \text{Tr}[U_1 U_3^\dagger] \text{Tr}[U_2^\dagger U_3] \\ &\quad - \frac{1}{2N_c} \text{Tr}[U_1 U_2^\dagger]. \end{aligned} \quad (4)$$

It is easy to see that the graphical representation of the color structure of this process is topologically equivalent to that shown in Fig. 6(b). As previously anticipated, the message to take from here is that the color flow structure present in this process is the same for both cases presented above for the leading part in the large- $N_c$  limit. Moreover, this is the same structure we see when only two gluons are present in the multiple scattering, which are always the product of two fundamental dipoles. As opposed to processes where gluons are emitted, no extra color charge is created at the vertex and therefore the color structure remains unchanged; the same is also true for processes with a quark-antiquark pair merging into a gluon, which might be important for higher-order contributions.

The observations above allow us to neglect—from the point of view of the color structure of the process in the large- $N_c$  limit—all of the vertices involving a gluon splitting into a quark-antiquark pair, and to focus our attention on processes where all of the vertices involve a quark

emitting a gluon or a gluon splitting into two gluons. The four-gluon vertex can also be ignored since its color structure is equivalent to a combination of three-gluon vertices.

Up until now, the large- $N_c$  limit has been mainly invoked to be able to regard color traces as separate entities—even after one takes the average over the background color field—arguing that correlations between fields entering Wilson lines in different color traces are suppressed by factors of  $1/N_c^2$ . The multiple-scattering factors of the processes considered so far, when expressed in terms of fundamental Wilson lines only, can all be expressed in terms of products of traces of either two or four Wilson lines in the fundamental representation. This will not be the case from now on when we start to consider more complicated processes, starting with the case of an initial gluon splitting into two gluons which fragment independently. This process will have contributions from diagrams with three and four gluons present at the moment of the multiple scattering, which will lead to traces of six and eight fundamental Wilson lines.

Let us consider first the case where the multiple scattering occurs after the splitting in the amplitude and before the splitting in the conjugate amplitude. It is easy to see that there are three gluons involved in the multiple scattering—each one contributing one adjoint Wilson line to the multiple-scattering factor—and that they are connected before and after the scattering by three-gluon vertices. Following Ref. [5], we can evaluate the relevant scattering matrices, which yield

$$\begin{aligned} f_{ade} W_1^{db} W_2^{ec} f_{fbc} W_3^{af} &= \frac{1}{2} \text{Tr}[U_1 U_3^\dagger] \text{Tr}[U_3 U_2^\dagger] \text{Tr}[U_2 U_1^\dagger] \\ &\quad + \frac{1}{2} \text{Tr}[U_2 U_3^\dagger] \text{Tr}[U_1 U_2^\dagger] \text{Tr}[U_3 U_1^\dagger] \\ &\quad - \frac{1}{2} \text{Tr}[U_3 U_2^\dagger U_1 U_3^\dagger U_2 U_1^\dagger] \\ &\quad - \frac{1}{2} \text{Tr}[U_1 U_2^\dagger U_3 U_1^\dagger U_2 U_3^\dagger]. \end{aligned} \quad (5)$$

The corresponding graphical representation is shown in Fig. 9. Finding the correct graphical representation—in terms of fermion lines only—without explicitly performing the algebra shown in Eq. (5) is possible as long as one knows how to represent two consecutive three-gluon vertices in the double-line representation. The identity to be used is illustrated in Fig. 10.



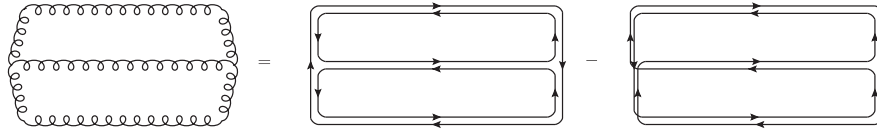


FIG. 9. The graphs on the right-hand side of the equation should also include their Hermitian conjugates, which can be obtained by simply reversing all of the arrows. Here all the correlators are assumed to be real, and therefore the  $\frac{1}{2}$  factor is cancelled.

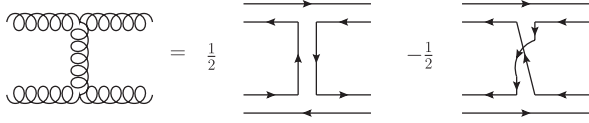


FIG. 10. Double-line representation of the gluon vertex. Here we should include the Hermitian conjugates of the graphs on the right-hand side of the equation.

Both Eq. (5) and Fig. 9 show that the term with a trace of six Wilson lines (sextupole) is suppressed in the large- $N_c$  limit. On the one hand, the terms with a product of three color traces are proportional to  $N_c^3$ , while the terms with only one trace are of order  $N_c$ . On the other hand, the graphical representation clearly shows that the term with the sextupole comes from a nonplanar diagram and therefore is suppressed with respect to planar diagrams by at least a factor of  $1/N_c^2$ .

The case where the multiple scattering occurs after the splitting, both in the amplitude and the conjugate amplitude, is treated similarly. Now, there is an extra gluon present in the multiple scattering, contributing an extra adjoint Wilson line, and the two three-gluon vertices are placed before the scattering. The color connections after the scattering are given by identifying the corresponding gluons from the amplitude and the conjugate amplitude. In summary, the relevant multiple-scattering term, in terms of adjoint Wilson lines as well as fundamental Wilson lines, is

$$\begin{aligned}
 & f_{ade}(W_1 W_2^\dagger)^{db} f_{abc}(W_3 W_4^\dagger)^{ec} \\
 &= \frac{1}{2} \text{Tr}[U_2 U_1^\dagger] \text{Tr}[U_3 U_4^\dagger] \text{Tr}[U_1 U_2^\dagger U_4 U_3^\dagger] \\
 &+ \frac{1}{2} \text{Tr}[U_4 U_3^\dagger] \text{Tr}[U_1 U_2^\dagger] \text{Tr}[U_3 U_4^\dagger U_2 U_1^\dagger] \\
 &- \frac{1}{2} \text{Tr}[U_2 U_1^\dagger U_3 U_4^\dagger U_1 U_2^\dagger U_4 U_3^\dagger] \\
 &- \frac{1}{2} \text{Tr}[U_1 U_2^\dagger U_3 U_4^\dagger U_2 U_1^\dagger U_4 U_3^\dagger]. \tag{6}
 \end{aligned}$$

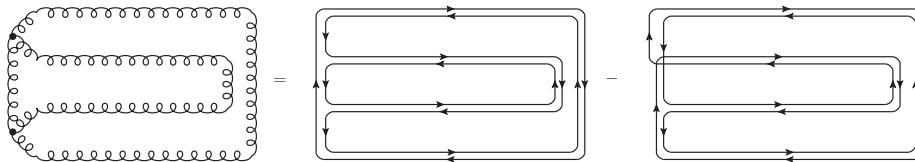


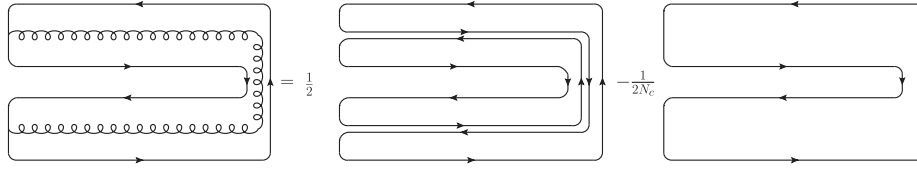
FIG. 11. The graphs on the right-hand side of the equation should also include their Hermitian conjugates, which can be obtained by simply reversing all of the arrows. Here all the correlators are assumed to be real, and therefore the  $\frac{1}{2}$  factor is cancelled.

Its graphical representation is given in Fig. 11, where once again we made use of the identity illustrated in Fig. 10. Similarly to the previous case, it is easy to see that the term with three color traces is the one that dominates in the large- $N_c$  limit, and the term with a trace of eight Wilson lines (octupole) is subleading. We can then safely state that, for all the cases considered in this section, the leading contribution to the multiple-scattering term in the large- $N_c$  limit can always be written in terms of dipole and quadrupole correlators only.

#### IV. THREE PARTICLES IN THE FINAL STATE

The aim of this section is to show with explicit examples how the color structure of a given process is affected by the inclusion of additional gluons in the final state. At the end of the previous section it was seen already that when the complexity of the problem increases—as well as the number of colored particles participating in the multiple scattering—it is natural that new higher-point correlations have to be included in the full description of the process. It was also seen that these higher-point correlations always appear suppressed by inverse powers of  $N_c$  when the multiple-scattering factor is expressed only in terms of fundamental Wilson lines. The same will be observed in the examples shown in this section: higher-point correlations keep appearing, but the leading term in the large- $N_c$  limit can always be written in terms of dipole and quadrupole amplitudes.

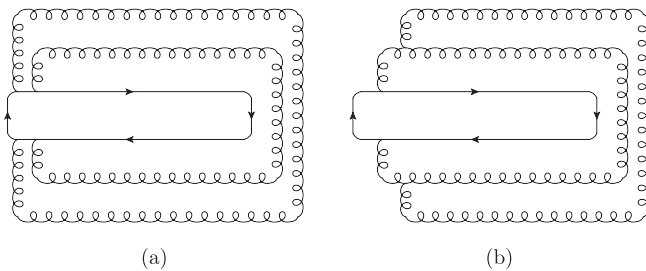
Let us start with one of the simplest cases at this level, which at the same time will show us a general feature of the further inclusion of gluons. Consider the process of production of a quark-antiquark pair and a gluon in DIS. As was observed in previous cases, it is sufficient to consider the case where the maximum number of particles participate in the multiple scattering since any other combination would yield simpler correlators. The process is then described by a photon splitting into a quark-antiquark

FIG. 12.  $q\bar{q}g$  production in DIS.

pair, which emits a gluon before undergoing multiple scatterings with the target field in both the amplitude and conjugate amplitude. The multiple-scattering term, therefore, includes two quark-antiquark pairs and two gluons with the color connections as shown in Fig. 12, and can be written as

$$\begin{aligned} & \text{Tr}[U_1^\dagger t^a U_2 U_4^\dagger t^b U_3](W_5 W_6^\dagger)^{ab} \\ &= \frac{1}{2} \text{Tr}[U_2 U_4^\dagger U_6 U_3^\dagger] \text{Tr}[U_3 U_1^\dagger U_5 U_6^\dagger] \\ & \quad - \frac{1}{2N_c} \text{Tr}[U_3 U_1^\dagger U_2 U_4^\dagger]. \end{aligned} \quad (7)$$

Both graphically and algebraically it is easy to see that the effect of adding a new gluon to the process studied in Sec. III C can be understood in terms of the Fierz identity. Here we choose to interpret the result in terms of the graphical representation. The extra gluon can be removed from the diagram by the rule depicted in Fig. 4, regardless of it being involved in the multiple interaction. For this particular case, the first term on the right-hand side of Fig. 4 cuts the already existing quadrupole in two, giving as a result a term with two color traces—which will clearly dominate in the large- $N_c$  limit—as compared to the second term, which does not introduce any new traces and has an extra factor of  $1/N_c$  in front. Here the original quadrupole is split into two quadrupoles, but it is easy to see that for slightly different cases—as for example if one considers the term with scattering before the emission of the gluon in the conjugate amplitude—one can end up with a quadrupole and a dipole. These small variations of the same process can be seen as attaching the gluon to different places of the original quadrupole. At the end of the day the result is always the same: the leading term in the large- $N_c$  limit will be given by the term that splits the original color trace into two different color traces.

FIG. 13.  $q \rightarrow qgg$ . (a) Additional gluon emitted from quark. (b) Additional gluon emitted from gluon.

Next, we switch our attention to processes present in  $pA$  collisions. First consider the quark-initiated process with one quark and two gluons in the final state. The relevant diagrams can all be obtained by considering all possible ways of attaching one extra gluon to the diagrams contributing to the  $q \rightarrow qg$  process. As an illustration, consider the diagrams corresponding to the square of the processes where the additional gluon is emitted either by the final quark or by the first gluon and all three particles participate in the interaction with the background field. The color structure is given by the diagrams of Fig. 13.<sup>1</sup> It is easy to see that for the case where the second gluon is emitted from the quark the color structure can be resolved by a straightforward application of the Fierz identity, leading to the conclusion that the leading term in the large- $N_c$  limit is given by one dipole and two quadrupoles. Instead of getting into the algebraic details of this computation, we choose the graphical approach here to show how the additional gluon modifies the structure of the correlator. Consider the diagram in the first term of the right-hand side of Fig. 3, representing the leading piece of the  $q \rightarrow qg$  process, and include the additional gluon as shown in Fig. 14. Since the gluon is only attached to the quadrupole part one can momentarily forget about the dipole part: it is clear that when one uses the Fierz identity to remove the gluon from the diagram one observes that the dominant piece of the diagram is the one in which the quadrupole is split into two quadrupoles.

For the case just described, there was no other choice but to attach the additional gluon to the quadrupole from the leading piece of the  $q \rightarrow qg$  process. When one considers other diagrams—such as the one already described where the second gluon is emitted from the first gluon—there are other ways of attaching this new gluon to the dominant part of the diagram. In general one can consider all possible ways of attaching the two legs of the new gluon and quickly realize that the pieces which will survive in the large- $N_c$  limit are the ones coming from attaching both legs of the new gluon to the same fermion loop. As an illustration, let us consider the algebraic expression of the scattering term for the diagram in Fig. 13(b):

<sup>1</sup>Here we are only interested in the planar diagrams, in which gluon lines do not cross one another. The nonplanar diagrams are large- $N_c$  suppressed, and thus are always discarded.

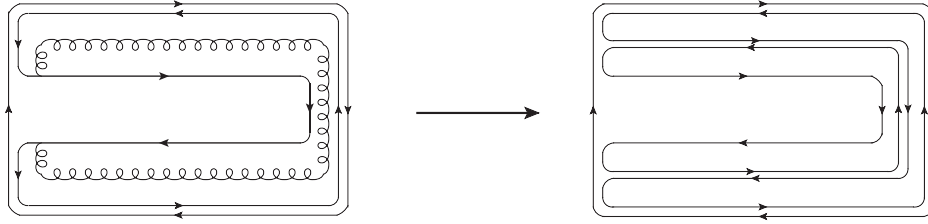


FIG. 14. Illustration of the effect of the extra gluon in the leading piece for one diagram contributing to the  $q \rightarrow qgg$  process.

$$\begin{aligned}
 & \text{Tr}[U_5^\dagger t^a t^{a'} U_6] f_{ade} (W_1 W_2^\dagger)^{db} f_{a'bc} (W_3 W_4^\dagger)^{ec} \\
 &= \frac{1}{4} \text{Tr}[U_1 U_2^\dagger U_4 U_3^\dagger] \text{Tr}[U_6 U_5^\dagger U_3 U_4^\dagger] \text{Tr}[U_2 U_1^\dagger] \\
 &+ \frac{1}{4} \text{Tr}[U_3 U_4^\dagger U_2 U_1^\dagger] \text{Tr}[U_6 U_5^\dagger U_1 U_2^\dagger] \text{Tr}[U_4 U_3^\dagger] \\
 &- \frac{1}{4} \text{Tr}[U_6 U_5^\dagger U_1 U_2^\dagger U_4 U_3^\dagger U_2 U_1^\dagger U_3 U_4^\dagger] \\
 &- \frac{1}{4} \text{Tr}[U_6 U_5^\dagger U_3 U_4^\dagger U_2 U_1^\dagger U_4 U_3^\dagger U_1 U_2^\dagger]. \quad (8)
 \end{aligned}$$

One can clearly see that the first two terms come from attaching the two legs of the new gluon to the same preexisting fermion loop, while the last two terms come from attaching the two legs of the new gluon to different fermion loops. Higher-point correlators appear in this expression but are always suppressed by a power of  $1/N_c^2$ , as compared to the terms with only dipoles and quadrupoles.

For the gluon-initiated processes the situation is very similar. Even though the explicit calculations are more intricate and tedious, one can easily recognize that the leading terms for large- $N_c$  for the process  $g \rightarrow ggg$  consist of a combination of two dipoles and two quadrupoles. One can perform a similar analysis to the one performed above for the  $q \rightarrow qgg$  process, starting with the leading piece of the  $g \rightarrow gg$  process and adding an extra gluon. Again, the terms that survive in the large- $N_c$  limit will be the ones coming from attaching both legs of the new gluon to only one of the preexisting fermion loops—in this case two dipoles and one quadrupole—therefore creating one extra quadrupole (in the case where all produced particles participate in the multiple scattering in both the amplitude and conjugate amplitude).

## V. PROOF OF THE GENERAL CASE

The argument used in the previous section to go from processes with two particles in the final state to processes with three particles in the final state can be generalized in a straightforward manner to an arbitrary number of particles in the final state. In order to do so in a consistent matter we will show by induction that adding a new particle to the final state does not change the fact that the leading terms in the large- $N_c$  limit are given in terms of only dipoles and quadrupoles. We find it convenient to focus first on the

leading order for a given number of particles, and then show how the argument can be further generalized to also include all-order contributions.

### A. Leading order

Before getting into the details of the inductive step of the proof, let us summarize some of the observations that have been made throughout the paper, which will be useful for the argument presented in this section.

- (1) In the large- $N_c$  limit, the  $N_c$  power counting is most easily done when scattering factors are expressed fully in terms of fundamental Wilson lines, where each trace contributes with a factor of  $N_c$ .
- (2) Changing the moment of the multiple interaction does not change the  $N_c$  power counting. The case where all the final-state particles participate in the multiple interaction is where the most complicated correlators can possibly be found, and therefore these will be the only cases under study in this section.
- (3) A gluon splitting into a quark-antiquark pair does not add any color charge to the process and therefore leaves its color structure unchanged. For the argument presented here one can neglect any new contributions from processes with extra quark-antiquark pairs in the final state and always assume that the additional particles are gluons.
- (4) From the point of view of the color structure only, a four-gluon vertex can always be represented by the sum of different ways of combining two three-gluon vertices. Because of this, processes with four-gluon vertices are not considered since its color structure is already accounted for by a proper treatment of the three-gluon vertices.

These observations reduce significantly the number of cases we have to consider to show that the inductive step in our proof indeed works. Suppose that all the correlators needed to describe all processes with  $k$  particles in the final state in the large- $N_c$  limit are dipoles and quadrupoles. Now consider a planar diagram for a process with  $k + 1$  particles in the final state: remove one gluon and consider the representation of the leading  $N_c$  piece of the remaining diagram in terms of only fundamental Wilson lines. Since it is a planar diagram corresponding to a process with

$k$  particles in the final state, its representation in terms of only fundamental Wilson lines is expressed in terms of dipoles and quadrupoles only. Now reattach the gluon removed in the previous step. There are two possibilities: either both of its legs are attached to the same fermion loop, or each leg is attached to a different fermion loop. In the first case, one can see from the examples in Sec. IV that the insertion of the new gluon splits the corresponding fermion loop—either dipole or quadrupole—creating a new quadrupole (when the new dipole interacts in both the amplitude and the conjugate amplitude—as was pointed out—any other case would lead to simpler correlators). The second case can be easily seen to be suppressed by a factor of  $1/N_c^2$  with respect to the first case. The two terms one obtains after applying the Fierz identity to a gluon joining two separate fermion loops have one power of  $N_c$  less compared to the diagram without the extra gluon; one of them has one loop less while the other has an explicit factor of  $1/N_c$ . This is to be compared to the first case where one additional fermion loop is created, and therefore one extra power of  $N_c$  is present.

We can therefore conclude that for any multiple-jet graphs, under the framework of saturation physics, the dipole and quadrupole are the only objects that appear in a physical multiple-jet production process in the large- $N_c$  limit. One should note that so far our proof does not apply to multiparticle production processes with large rapidity intervals or gaps between the measured particles (all jets are produced in the same rapidity region). For such situations, one needs to consider higher-order diagrams (and at least re-sum those that contain a logarithmic enhancement). In the following section, we explain that our proof holds to all orders in  $\alpha_s$ , which encompasses those situations where particles are emitted with large rapidity differences.

### B. Higher-order $\alpha_s$ corrections

As briefly mentioned earlier, within the framework of the dilute-dense factorization, the next-to-leading order  $\alpha_s$  corrections of the single inclusive production cross sections [25] in the large- $N_c$  limit do not involve higher-point functions. Here we would like to generalize this conclusion up to all order. There are two classes of graphs at higher order, namely, the virtual graphs and real graphs. In terms of color structure in the coordinate space, these two classes of graphs are actually similar. They both introduce an additional gluon at a new coordinate. The only difference is that the additional gluon in the real graphs goes through a cut and is produced in the final state. For the real graphs, we can follow the above discussion on the multiple-jet productions, and integrate over an arbitrary number of final-state jets and arrive at the conclusion that all real graphs in the large- $N_c$  limit can only involve dipoles and quadrupoles. For the virtual graphs, we can easily see that the large- $N_c$  limit requires the additional gluon within a

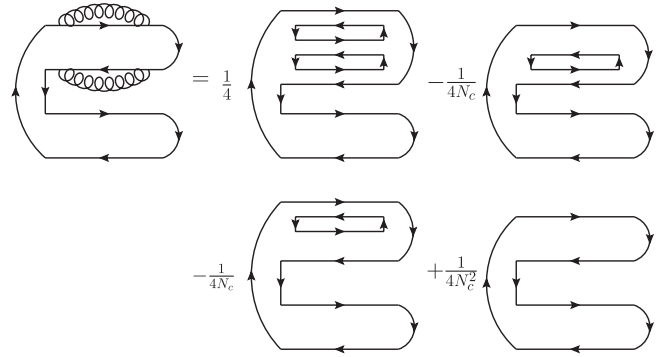


FIG. 15. Higher-order  $\alpha_s$  contribution to the  $q\bar{q}$  dijet.

dipole or a quadrupole, and thus higher-order virtual graphs can only generate more dipoles. Let us take the DIS dijet as an example, where we add a one-gluon loop in both the amplitude and complex conjugate amplitude, as shown in Fig. 15. Using the Fierz identity, it is obvious that the addition of the virtual gluons in the dijet processes does not introduce higher-point functions in the large- $N_c$  limit.

We have shown that, to all orders in  $\alpha_s$ , all multiparticle production processes in dilute-dense collisions are expressible in terms of dipoles and quadrupoles only in the large- $N_c$  limit. In particular, this includes the case where particles are emitted with a large rapidity difference, along with un-tagged emissions or gaps in between. We would like to point out that, in the case of strongly ordered gluon emissions, this result was first obtained in Ref. [37]. Our derivation extends the result to the general case of noneikonal gluon, quark, or antiquark emissions.

## VI. CONCLUSION

In conclusion, we find that in the large- $N_c$  limit, all multiparticle production processes in p + A-type collisions up to all orders in  $\alpha_s$  can be described in terms of only dipoles and quadrupoles under the color glass condensate framework, excluding cases with large rapidity intervals or gaps between the measured particles. This conclusion can very possibly lead us to an effective  $k_t$  factorization at small  $x$  for multiple-jet production processes in high-energy scatterings within a dilute-dense system. This effective  $k_t$  factorization involves two fundamental objects, namely, the dipole and the quadrupole, and it can only work in the large- $N_c$  limit. Only in the large- $N_c$  limit can one get rid of all of the higher-point functions, which are presumably new objects. Provided we understand both dipoles and quadrupoles well, we will be able to predict any multiple-jet production processes up to corrections of order  $\frac{1}{N_c^2}$  by using this effective  $k_t$  factorization.

## ACKNOWLEDGMENTS

We thank F. Gelis, A. Kovner, A.H. Mueller, R. Venugopalan, and F. Yuan for discussions and comments.



This work was supported in part by the U.S. Department of Energy under the contracts DOE OJI Grant No. DE-SC0002145 and Polish NCN Grant No. DEC-2011/01/B/ST2/03915. F. D.'s research is supported by the European Research Council under the Advanced Investigator Grant ERC-AD-267258. C. M.'s research is supported by the European Research Council Grant HotLHC ERC-2011-StG-279579. A. M. S. is supported by the Sloan Foundation.

### APPENDIX: LARGE- $N_c$ EVALUATION OF CORRELATORS IN THE MCLERRAN-VENUGOPALAN MODEL

In this appendix we show how one can compute general  $n$ -point correlators under the framework of the McLerran-Venugopalan model [38] in the large- $N_c$  limit. The formalism we will employ is the one introduced in Refs. [39,40], which has also been successfully used to compute the full finite- $N_c$  expressions for several correlators in Refs. [5,41–43].

$$M = \begin{pmatrix} C_F(L_{x_1x_2} + L_{x'_2x'_1}) + \frac{1}{2N_c} F(x_1, x_2; x'_2, x'_1) & -\frac{1}{2} F(x_1, x'_1; x'_2, x_2) \\ -\frac{1}{2} F(x_1, x_2; x'_2, x'_1) & C_F(L_{x_1x'_1} + L_{x'_2x_2}) + \frac{1}{2N_c} F(x_1, x'_1; x'_2, x_2) \end{pmatrix}, \quad (\text{A2})$$

with  $F(x_1, x_2; x'_2, x'_1) = L_{x_1x'_2} - L_{x_1x'_1} + L_{x_2x'_1} - L_{x_2x'_2}$ .

If one naively takes the large- $N_c$  limit the matrix becomes diagonal, which is consistent with the fact that each color transition is suppressed by a factor of  $1/N_c^2$ . For correlators where the singlet structure is not the same at both ends of the longitudinal extent, it is not appropriate to take the large- $N_c$  limit at the level of the transition matrix since different singlet states receive different weights in the final calculation. For example, for the quadrupole calculation in Ref. [5] one can see that the relevant combination of matrix elements for the  $n$ th-order term of the expansion takes the form  $(M^n)_{11} + N_c(M^n)_{21}$ , where the nondiagonal component appears multiplied by a factor of  $N_c$ .

One can see from the explicit expression for the matrix  $M$  that  $M_{11}$  and  $M_{22}$  have one additional factor of  $N_c$  when compared to  $M_{12}$  and  $M_{21}$ . When taking the leading  $N_c$  term of the elements of  $M^n$  it is easy to see that  $(M^n)_{11} = M_{11}^n$  and  $(M^n)_{22} = M_{22}^n$ , while  $(M^n)_{21}$  includes only terms with one factor of  $M_{21}$  and  $n - 1$  factors of  $M_{11}$  or  $M_{22}$ , which is the same as taking  $M_{12} = 0$  right from the beginning ( $M_{11}$  and  $M_{22}$  can also be replaced by their large- $N_c$  versions). The fact that the nondiagonal element enters only once signals that there was only one color transition.

One can easily see that

$$(M^n)_{21} = M_{21} \sum_{k=0}^{n-1} M_{11}^k M_{22}^{n-k-1} = M_{21} \frac{M_{11}^n - M_{22}^n}{M_{11} - M_{22}}. \quad (\text{A3})$$

The general strategy consists in expanding the Wilson lines, and then taking advantage of the fact that the only nontrivial correlation is the average of two gauge fields by using Wick's theorem. The elementary correlator of two fields takes the form

$$g_S^2 \langle A_c^-(z^+, x) A_d^-(z'^+, y) \rangle_{x_g} = \delta_{cd} \delta(z^+ - z'^+) \mu_{x_g}^2(z^+) L_{xy}, \quad (\text{A1})$$

where  $L_{xy}$  can be written in terms of a two-dimensional massless propagator (see Ref. [5]). In order to be able to re-sum these two-point contractions it is necessary to pay close attention to the color algebra. Only overall singlet states need to be considered: one can therefore calculate the matrix indicating the possible transitions between such states, and then diagonalize it.

This was done explicitly for correlators involving four fundamental Wilson lines (two quark-antiquark pairs) in Refs. [5,40,41], where only two overall singlet states are available and the corresponding transition matrix takes the following form:

One must perform an ordered integral of the longitudinal coordinates and then sum over  $n$ . Since in a McLerran-Venugopalan-like Gaussian model the longitudinal dependence of the correlations factors out, the ordered integral is equal to  $\frac{1}{n!}$  times the full integral. From there it is easy to see that the  $n$ th powers appearing above become exponentials and the large- $N_c$  formula for the quadrupole is recovered.

This way of taking the large- $N_c$  limit at the matrix level can be generalized to more complicated correlators, with similar results. One can find an ordering of the singlet states such that all the information necessary to find the large- $N_c$  version of the correlator is in a lower diagonal matrix organized in blocks, in which going away from the diagonal lowers the power of  $N_c$  of the corresponding matrix element. Here we describe this procedure for the case of the six-point correlator of the form  $\frac{1}{N_c} \langle \text{Tr}(U_1 U_2^\dagger U_3 U_4^\dagger U_5 U_6^\dagger) \rangle$ .

For such a system of three quarks and three antiquarks there are six singlet states available, corresponding to the six ways of pairing quarks with antiquarks. The proper way to organize the states in the matrix representation is according to the power of  $N_c$  of the overlap with the final singlet state. In terms of the graphical representation introduced in Ref. [40], the six singlet states correspond, in that particular order, to the topologies shown in Fig. 16, where the number of fermion loops gives the power of  $N_c$  associated with the overlap.

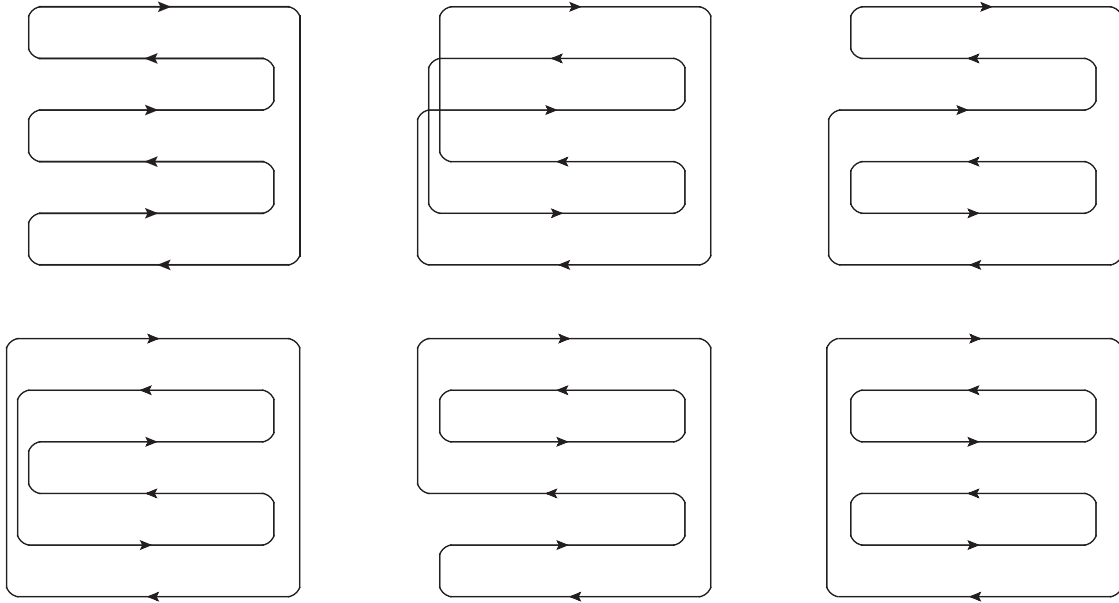


FIG. 16. Graphical representation of the six topologies involved in the calculation. The power of  $N_c$  associated with each configuration is equal to the number of fermion loops.

In the large- $N_c$  limit only transitions to states corresponding to a higher power of  $N_c$  are allowed, which—thanks to the specific order chosen for the singlet states—means that one can divide the corresponding transition matrix into blocks, and all of the blocks above the diagonal can be neglected. The corresponding transition matrix  $M$  then takes the following form:

$$M = \begin{pmatrix} M_1 & 0 & 0 \\ M_4 & M_2 & 0 \\ 0 & M_5 & M_3 \end{pmatrix}, \quad (\text{A4})$$

where the matrices along the diagonal are diagonal, and the off-diagonal matrices have one power of  $N_c$  less than the ones along the diagonal. It is not difficult to calculate the  $n$ th power of this matrix:

$$M^n = \begin{pmatrix} M_1^n & 0 & 0 \\ \sum_{i=0}^{n-1} M_2^i M_4 M_1^{n-i-1} & M_2^n & 0 \\ \sum_{i=0}^{n-2} \sum_{j=0}^{n-i-2} M_3^i M_5 M_2^j M_4 M_1^{n-i-j-2} & \sum_{i=0}^{n-1} M_3^i M_5 M_2^{n-i-1} & M_3^n \end{pmatrix}. \quad (\text{A5})$$

One can easily see that the relevant matrix elements for the evaluation of the desired correlator are of the form

$$(1 \ 1 \ N_c \ N_c \ N_c \ N_c^2) M^n \begin{pmatrix} 1 \\ 0 \\ 0 \\ 0 \\ 0 \\ 0 \end{pmatrix}. \quad (\text{A6})$$

This singles out the first column of  $M^n$ . Since  $M_1$  and  $M_2$  are diagonal matrices it is easy to see that the elements of  $M$  in the second column never enter the expressions for

the elements of  $M^n$  in the first column. Following this observation, we drop completely all contributions from the second column (and second row), which correspond to the second topology proportional to  $N_c$ .

As a  $5 \times 5$  matrix,  $M$  has the form

$$M = \begin{pmatrix} m_{11} & 0 & 0 & 0 & 0 \\ m_{21} & m_{22} & 0 & 0 & 0 \\ m_{31} & 0 & m_{33} & 0 & 0 \\ m_{41} & 0 & 0 & m_{44} & 0 \\ 0 & m_{52} & m_{53} & m_{54} & m_{55} \end{pmatrix}. \quad (\text{A7})$$

The first column of its  $n$ th power is

$$\left( \begin{array}{c} m_{11}^n \\ m_{21} \sum_{i=0}^{n-1} m_{11}^i m_{22}^{n-i-1} \\ m_{31} \sum_{i=0}^{n-1} m_{11}^i m_{33}^{n-i-1} \\ m_{41} \sum_{i=0}^{n-1} m_{11}^i m_{44}^{n-i-1} \\ \sum_{k=2}^4 m_{5k} m_{k1} \left[ \sum_{i=0}^{n-2} \sum_{j=0}^{n-i-2} m_{11}^i m_{kk}^j m_{55}^{n-i-j-2} \right] \end{array} \right), \quad (\text{A8})$$

which can be rewritten as

$$\left( \begin{array}{c} m_{11}^n \\ \frac{m_{21}}{m_{11}-m_{22}} [m_{11}^n - m_{22}^n] \\ \frac{m_{31}}{m_{11}-m_{33}} [m_{11}^n - m_{33}^n] \\ \frac{m_{41}}{m_{11}-m_{44}} [m_{11}^n - m_{44}^n] \\ \sum_{k=2}^4 m_{5k} m_{k1} \left[ \frac{m_{11}^n}{(m_{11}-m_{kk})(m_{11}-m_{55})} + \frac{m_{kk}^n}{(m_{kk}-m_{11})(m_{kk}-m_{55})} + \frac{m_{55}^n}{(m_{55}-m_{kk})(m_{55}-m_{11})} \right] \end{array} \right). \quad (\text{A9})$$

Now, as in the previous case, these expressions appear in the final result summed over  $n$  with a factor of  $\frac{1}{n!}$  due to the ordering in the longitudinal coordinate. Therefore the  $n$ th powers become exponentials.

One can easily calculate explicitly the relevant leading- $N_c$  piece of the transition matrix for the case of interest. This reduced version of the transition matrix then takes the form

$$M = \frac{1}{2} \left( \begin{array}{ccccc} N_c(L_{12} + L_{34} + L_{56}) & 0 & 0 & 0 & 0 \\ F_{1243} & N_c(L_{14} + L_{32} + L_{56}) & 0 & 0 & 0 \\ F_{1265} & 0 & N_c(L_{16} + L_{34} + L_{52}) & 0 & 0 \\ F_{3465} & 0 & 0 & N_c(L_{12} + L_{36} + L_{54}) & 0 \\ 0 & F_{1465} & F_{2534} & F_{1263} & N_c(L_{16} + L_{32} + L_{54}) \end{array} \right), \quad (\text{A10})$$

where  $F_{ijkl} = L_{ik} - L_{jk} + L_{jl} - L_{il}$ . By plugging these matrix elements back into the above equations, transforming the  $n$ th powers into exponentials, and including the tadpole contributions, one gets

$$\begin{aligned} \frac{1}{N_c} \langle \text{Tr}[U_1 U_2^\dagger U_3 U_4^\dagger U_5 U_6^\dagger] \rangle &= e^{-\Gamma_{12}-\Gamma_{34}-\Gamma_{56}} - \frac{F_{1234}}{F_{1324}} [e^{-\Gamma_{12}-\Gamma_{34}} - e^{-\Gamma_{14}-\Gamma_{32}}] e^{-\Gamma_{56}} \\ &- \frac{F_{1256}}{F_{1526}} [e^{-\Gamma_{12}-\Gamma_{56}} - e^{-\Gamma_{16}-\Gamma_{52}}] e^{-\Gamma_{34}} - \frac{F_{3456}}{F_{3546}} [e^{-\Gamma_{34}-\Gamma_{56}} - e^{-\Gamma_{36}-\Gamma_{54}}] e^{-\Gamma_{12}} \\ &+ F_{1234} F_{1456} \left[ \frac{e^{-\Gamma_{12}-\Gamma_{34}-\Gamma_{56}}}{F_{1324} G} - \frac{e^{-\Gamma_{14}-\Gamma_{32}-\Gamma_{56}}}{F_{1324} F_{1546}} + \frac{e^{-\Gamma_{16}-\Gamma_{32}-\Gamma_{54}}}{F_{1546} G} \right] \\ &+ F_{1256} F_{2543} \left[ \frac{e^{-\Gamma_{12}-\Gamma_{34}-\Gamma_{56}}}{F_{1526} G} - \frac{e^{-\Gamma_{16}-\Gamma_{34}-\Gamma_{52}}}{F_{1526} F_{2453}} + \frac{e^{-\Gamma_{16}-\Gamma_{32}-\Gamma_{54}}}{F_{2453} G} \right] \\ &+ F_{3456} F_{1236} \left[ \frac{e^{-\Gamma_{12}-\Gamma_{34}-\Gamma_{56}}}{F_{3546} G} - \frac{e^{-\Gamma_{12}-\Gamma_{36}-\Gamma_{54}}}{F_{3546} F_{1326}} + \frac{e^{-\Gamma_{16}-\Gamma_{32}-\Gamma_{54}}}{F_{1326} G} \right], \end{aligned} \quad (\text{A11})$$

where  $\Gamma_{ij} = \mu^2(L_{ii} + L_{jj} - 2L_{ij})$  and  $G = L_{12} + L_{34} + L_{56} - L_{16} - L_{32} - L_{54}$ .

In this expression one can easily recognize three different types of contributions, depending on the number of transitions between the singlet states. The first term clearly comes from the first row in Eq. (A9) and corresponds to the totally elastic part with no color transitions, the following three terms come from the second, third, and fourth rows of Eq. (A9) and correspond to terms with only one transition, and the rest of the terms come from the last row of Eq. (A9) and are associated with terms that have two transitions between singlet states.

- [1] A. Kovner and U. A. Wiedemann, *Phys. Rev. D* **64**, 114002 (2001).
- [2] F. Gelis, E. Iancu, J. Jalilian-Marian, and R. Venugopalan, *Annu. Rev. Nucl. Part. Sci.* **60**, 463 (2010).
- [3] J. Jalilian-Marian and Y. V. Kovchegov, *Phys. Rev. D* **70**, 114017 (2004); **71**, 079901E (2005).
- [4] C. Marquet, *Nucl. Phys.* **A796**, 41 (2007).
- [5] F. Dominguez, C. Marquet, B.-W. Xiao, and F. Yuan, *Phys. Rev. D* **83**, 105005 (2011).
- [6] F. Dominguez, A. H. Mueller, S. Munier, and B. W. Xiao, *Phys. Lett. B* **705**, 106 (2011).
- [7] A. Dumitru and J. Jalilian-Marian, *Phys. Rev. D* **82**, 074023 (2010).
- [8] E. Iancu and D. N. Triantafyllopoulos, *J. High Energy Phys.* **11** (2011) 105; **04** (2012) 025.
- [9] A. Dumitru, J. Jalilian-Marian, T. Lappi, B. Schenke, and R. Venugopalan, *Phys. Lett. B* **706**, 219 (2011).
- [10] A. H. Mueller, [arXiv:hep-ph/0111244](https://arxiv.org/abs/hep-ph/0111244).
- [11] A. H. Mueller, *Nucl. Phys.* **B335**, 115 (1990); **B415**, 373 (1994).
- [12] L. D. McLerran and R. Venugopalan, *Phys. Rev. D* **59**, 094002 (1999).
- [13] Y. V. Kovchegov and L. D. McLerran, *Phys. Rev. D* **60**, 054025 (1999); **62**, 019901E (2000).
- [14] A. H. Mueller, *Nucl. Phys.* **B558**, 285 (1999).
- [15] C. Marquet, B.-W. Xiao, and F. Yuan, *Phys. Lett. B* **682**, 207 (2009).
- [16] I. Arsene *et al.* (BRAHMS Collaboration), *Phys. Rev. Lett.* **93**, 242303 (2004).
- [17] J. Adams *et al.* (STAR Collaboration), *Phys. Rev. Lett.* **97**, 152302 (2006).
- [18] A. Dumitru and J. Jalilian-Marian, *Phys. Rev. Lett.* **89**, 022301 (2002).
- [19] Y. V. Kovchegov and A. H. Mueller, *Nucl. Phys.* **B529**, 451 (1998).
- [20] A. Dumitru and L. D. McLerran, *Nucl. Phys.* **A700**, 492 (2002).
- [21] Y. V. Kovchegov and K. Tuchin, *Phys. Rev. D* **65**, 074026 (2002).
- [22] C. Marquet, *Nucl. Phys.* **B705**, 319 (2005).
- [23] A. Dumitru, A. Hayashigaki, and J. Jalilian-Marian, *Nucl. Phys.* **A765**, 464 (2006).
- [24] T. Altinoluk and A. Kovner, *Phys. Rev. D* **83**, 105004 (2011).
- [25] G. A. Chirilli, B.-W. Xiao, and F. Yuan, *Phys. Rev. Lett.* **108**, 122301 (2012); G. A. Chirilli, B.-W. Xiao, and F. Yuan, *Phys. Rev. D* **86**, 054005 (2012).
- [26] A. H. Mueller and S. Munier, *Nucl. Phys.* **A893**, 43 (2012).
- [27] F. Dominguez, B.-W. Xiao, and F. Yuan, *Phys. Rev. Lett.* **106**, 022301 (2011).
- [28] F. Gelis and J. Jalilian-Marian, *Phys. Rev. D* **67**, 074019 (2003).
- [29] E. Braidot for the STAR collaboration, [arXiv:1005.2378](https://arxiv.org/abs/1005.2378).
- [30] A. Adare *et al.* (PHENIX Collaboration), *Phys. Rev. Lett.* **107**, 172301 (2011).
- [31] B.-W. Xiao and F. Yuan, *Phys. Rev. Lett.* **105**, 062001 (2010); *Phys. Rev. D* **82**, 114009 (2010).
- [32] N. N. Nikolaev, W. Schafer, B. G. Zakharov, and V. R. Zoller, *Phys. Rev. D* **72**, 034033 (2005).
- [33] R. Baier, A. Kovner, M. Nardi, and U. A. Wiedemann, *Phys. Rev. D* **72**, 094013 (2005).
- [34] J. L. Albacete and C. Marquet, *Phys. Rev. Lett.* **105**, 162301 (2010).
- [35] A. Stasto, B.-W. Xiao, and F. Yuan, *Phys. Lett. B* **716**, 430 (2012).
- [36] T. Lappi and H. Mäntysaari, [arXiv:1209.2853](https://arxiv.org/abs/1209.2853).
- [37] A. Kovner and M. Lublinsky, *J. High Energy Phys.* **11** (2006) 083.
- [38] L. D. McLerran and R. Venugopalan, *Phys. Rev. D* **49**, 2233 (1994); **49**, 3352 (1994).
- [39] H. Fujii, *Nucl. Phys.* **A709**, 236 (2002).
- [40] J. P. Blaizot, F. Gelis, and R. Venugopalan, *Nucl. Phys.* **A743**, 57 (2004).
- [41] F. Dominguez, C. Marquet, and B. Wu, *Nucl. Phys.* **A823**, 99 (2009).
- [42] Y. V. Kovchegov, J. Kuokkanen, K. Rummukainen, and H. Weigert, *Nucl. Phys.* **A823**, 47 (2009).
- [43] C. Marquet and H. Weigert, *Nucl. Phys.* **A843**, 68 (2010).